



Hydrophilic solvent recovery from switched-on microdroplet dissolution

Romain Billet¹ | Binglin Zeng¹  | Hongyan Wu¹ | James Lockhart² |
Mike Gattrell² | Hongying Zhao² | Xuehua Zhang¹ 

¹Department of Chemical and Materials Engineering, University of Alberta, Edmonton, Alberta, Canada

²BC Research Inc., Richmond, British Columbia, Canada

Correspondence

Hongying Zhao, BC Research Inc., Richmond, BC V6V 1M8, Canada.

Email: hzhao@bcrci.ca

Xuehua Zhang, Department of Chemical and Materials Engineering, University of Alberta, Edmonton, AB T6G 1H9, Canada.

Email: xuehua.zhang@ualberta.ca

Funding information

Mitacs Accelerate Program, Canada Foundation for Innovation; Natural Science and Engineering Research Council of Canada; Alberta-innovates; Canada Research Chairs program

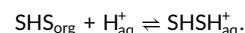
Abstract

Switchable hydrophilicity solvents (SHSs) are a unique class of chemical compounds that can be switched between their hydrophobic and hydrophilic forms. The switchable characteristics allow SHSs to be used as emerging, green solvents for sustainable extraction and separation technology. In the production of polymeric microparticles from recycled plastics, SHSs are used to dissolve the polymer and then are switched to the hydrophilic form for separation from the generated polymeric microparticles. However, it is extremely difficult to fully recover the SHS residue from the mixtures. In this work, we will identify the key parameters that determine the level of the solvent residue during the switched-on dissolution of emulsion microdroplets. The SHS *N,N*-dimethylcyclohexylamine from solvent-polymer binary emulsion droplets was switched to the hydrophilic, water-soluble form, triggered by addition of an acid in the surrounding aqueous phase. By applying a sensitive detection method developed in this work, we compared the levels of SHS residue in polymer microparticles obtained under 30 different dynamical and chemical conditions for the switching processes. The quantitative analysis revealed that residue levels remained constant at varied addition rates and concentration of the trigger solution, but decreased with the increase in organic phase fractions or the decrease in the emulsion temperature. Trapped water in the drops during switched-on dissolution may have contributed to the high level of solvent residue. The understanding of the new possible mechanism for residual solvent reported in this work may help develop effective approaches for the recovery of switchable solvents in environmentally friendly separation processes.

INTRODUCTION

Switchable hydrophilicity solvents (SHSs) are a unique family of solvents that are insoluble in water in their neutral form.^{1,2} However, on coming into contact with a trigger in water, such as CO₂, the SHS switches from its neutral insoluble form to a protonated soluble form.

The switch between the two forms is reversible, and consequently, the SHS can be recycled by removing CO₂ from the water. A general mechanism driving the switching process of SHSs is an acid–base (trigger) reaction:



Romain Billet and Binglin Zeng contributed equally to this study.

This is an open access article under the terms of the Creative Commons Attribution License, which permits use, distribution and reproduction in any medium, provided the original work is properly cited.

© 2023 The Authors. *Droplet* published by Jilin University and John Wiley & Sons Australia, Ltd.

Apart from using CO_2 to generate carbonic acid in water,³⁻⁵ some common triggers that have been used to switch SHSs include HCl ,⁶⁻⁸ H_2SO_4 , and H_3PO_4 .⁹ Note that a reverse approach to SHSs can also be accomplished with fatty acids, in which case a base like Na_2CO_3 can be used to initiate switching.^{10,11}

The switching characteristic makes SHSs ideal green alternatives to volatile organic compounds (VOCs) in separation and extraction technology. In a typical process, the SHS is used to separate a targeted chemical from another phase. The SHS is then removed from the product by switching the SHS in the presence of the trigger and water (hydrophobic to hydrophilic) to recover the separated compound and recycle SHS. Such applications have been demonstrated in oil extraction,¹²⁻¹⁴ extraction of lipids or other compounds from microalgae¹⁵⁻¹⁷ or extraction of phenols from lignin pyrolysis oil.¹⁸ However, one of the challenges is how to remove all the solvent residue from the product, as the residues often adversely impact the properties and purity of the product and also result in a loss of the switchable solvents from the process. The residual solvent is considered one of the challenges that hinders industrial applications.

The amount of residual solvent may depend on the type of SHS and the extracted compound, but also on extraction conditions such as water content, temperature, or stirring conditions. In polystyrene recycling, 8 wt% of the SHS *N,N*-dimethylcyclohexylamine (DMCHA) was found in the polystyrene phase.² Lower, but still significant residual solvent was found during multilayer packaging recycling, with 1-4 wt% of DMCHA in the low-density polyethylene phase¹⁹ and during poly(butyl methacrylate) latex formation, with around 2.5 wt% residue of another switchable solvent DMCHA (C_2NMe).²⁰ In viscous heavy oil extraction using DMCHA, approximately 12 wt% residue was found in the extracted oil, which can be reduced to 8 wt% under strong stirring conditions.¹⁴ A similar extraction with another SHS yielded residual content of up to 17 wt% with high water content.²¹ The residue level may depend on the extraction temperature. For example, 4-8 wt% of DMCHA was observed in lipid extraction from microalgae at room temperature and 18-24 wt% at higher temperatures.¹⁵

The problem of residual SHS in a product also poses a problem for the production of polymer microparticles using SHSs. Polymer microparticles are used in numerous applications, such as for the manufacture of gloves,²² paints,²³ or coatings.²⁴ These microparticles may be prepared from recycled plastics. However, the presence of residual SHS in polymer microparticles may lead to changes in the physical and chemical properties of the particles, affecting their performance and potentially posing health risks if used in medical applications. SHS removal has been shown to work effectively for the formation of different polymer microparticles via emulsion switching of C_2NMe including natural rubber, poly(methyl methacrylate), poly(ethyl methacrylate), and polystyrene.²⁰

To date, the predominant strategy used to reduce the solvent residue has been to expand the range of SHSs to find more efficient solvents.^{25,26} Tertiary amines are the most widely used category of SHS,^{2,27} but recent work has expanded the solvents to diamines with improved phase behavior²⁸ or amine-free SHS.²⁹

In this work, we focus on the effects of switching conditions on the amount of residual solvent in polymer microparticles. We found a constant level of the solvent residue in the final polystyrene particles regardless of the addition rate and solution concentration of the trigger. However, a decrease in the solvent residue was achieved at higher fractions of the organic dispersed phase in the emulsion or at lower extraction temperatures. The solvent residue may be attributed to the formation of a water-oil-water emulsion during the extraction process, in addition to the trapped solvent by concentrated polymer near the end of the emulsion extraction. These findings have significant implications for the recycling of SHS in the production of microparticles and may lead to the development of effective approaches for reducing the solvent residue.

RESULTS AND DISCUSSION

An initial goal was to establish a sensitive method for the quantification of DMCHA residue in solid polystyrene (PS) particles. To do this, the PS prepared from emulsion extraction was first dissolved into toluene, then DMCHA was extracted from the PS and toluene solution to an acidic aqueous phase, as shown in Figure 1. Following this, the amount of extracted DMCHA was quantified using Raman spectroscopy and a reference calibration curve.

To establish a calibration curve, a controlled amount of pure DMCHA is injected in a fixed amount of toluene. The SHS is then extracted using a 0.9 M sulfuric acid solution, and the pH can be easily adjusted by modulating the acidic concentration. The aqueous phase is then analyzed by Raman spectroscopy. The extraction is repeated several times with different amounts of DMCHA injected in the toluene phase.

Figure 1c shows the Raman spectra of the aqueous phase after extraction with 10-90 mg of DMCHA in the toluene phase, corresponding to a DMCHA concentration of 0.3-2.7 g/L. The most prominent peaks in Raman spectra situated at 440, 590, 890, 982, and 1050 cm^{-1} can be attributed to sulfuric acid, the most abundant compound in the solution. In previous work on Raman spectroscopy of sulfuric acid solutions,³⁰⁻³² the 890 cm^{-1} peak was attributed to the asymmetric stretching vibration of HSO_4^- , while the 982 and 1050 cm^{-1} peaks were attributed, respectively, to the symmetric stretching vibration of HSO_4^- and SO_4^{2-} .

Figure 1d shows an enlargement of the peak situated at 778 cm^{-1} , the characteristic peak of extracted DMCHA. The peak at 778 cm^{-1} does not appear without DMCHA, while the intensity is correlated with the concentration of DMCHA injected in the toluene solution. Previous work assigned the peaks in the spectral range from 400 to 1600 cm^{-1} in *N,N*-dimethylaniline (DMA) to the vibration modes of the ring.^{33,34} As the molecular structure of DMA is similar to that of DMCHA, the characteristic peak at 778 cm^{-1} can be assigned to a vibration mode of the ring in DMCHA.

Figure 1e shows the intensity of the peak at 778 cm^{-1} against the concentration of DMCHA in the toluene solution. The intensity of the

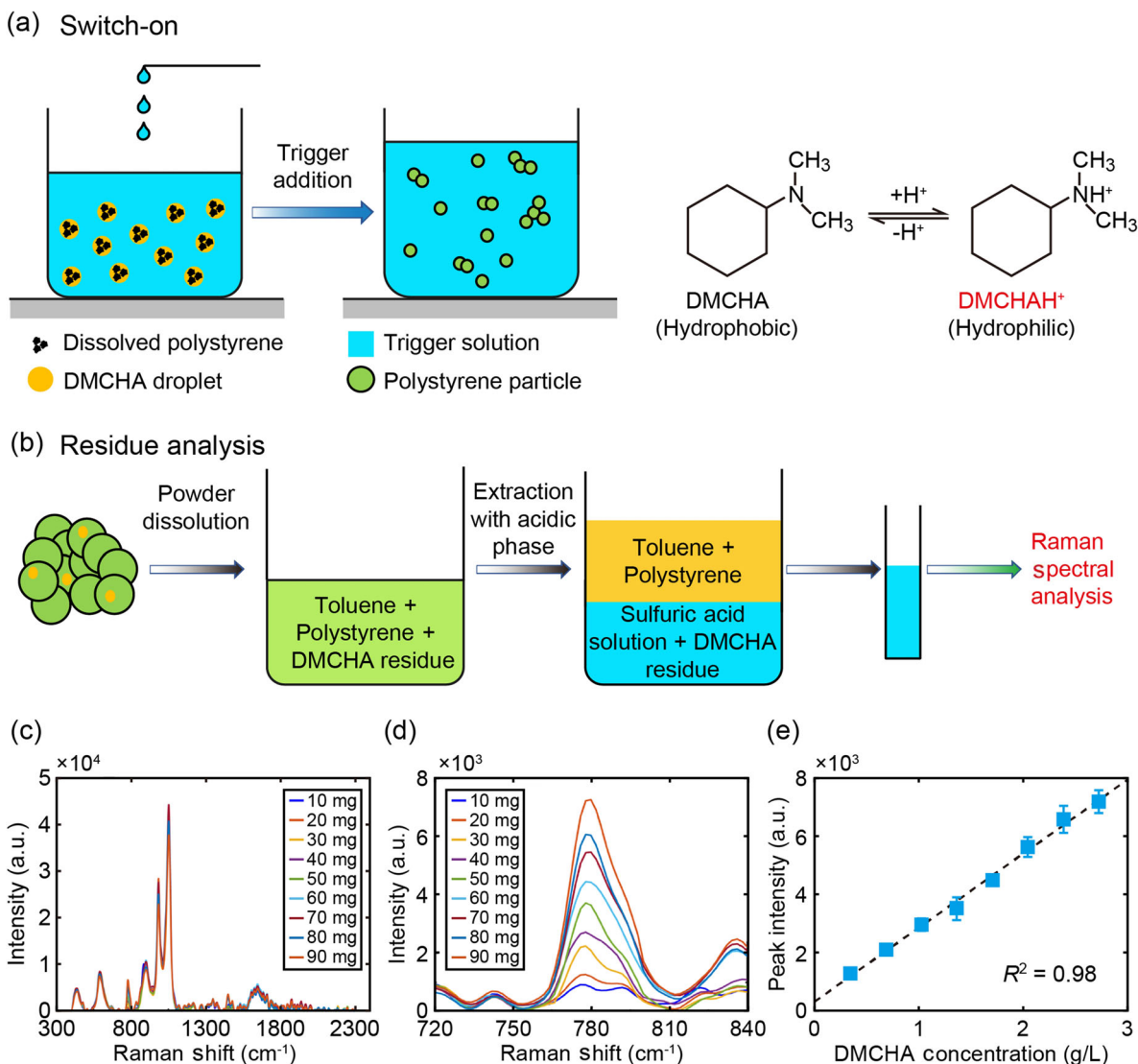


FIGURE 1 Switch-on dissolution and solvent residue analysis. (a) Schematic depiction of the emulsion switching process. An emulsion of DMCHA/polystyrene in water is placed in a container, and an acidic trigger solution is then added at a fixed rate. DMCHA in the SHS/polymer drops is switched to its hydrophilic form and solubilized in the surrounding aqueous environment, leaving only polystyrene as microparticles. (b) Residual DMCHA extraction from microparticles obtained from the DMCHA/polystyrene emulsion drop dissolution. The powder of microparticles is dissolved in toluene. An acidic aqueous phase is then added and mixed to extract the residual DMCHA. The aqueous phase is then transferred out for Raman spectroscopic analysis. (c) Raman spectra of the extractant aqueous phase after the extraction process for DMCHA mass from 10 to 90 mg injected in the toluene phase. (d) Zoomed view of the DMCHA characteristic peak at 778 cm^{-1} . An increased amount of DMCHA in the toluene phase results in an increase in the intensity of the peak. (e) Plot of the measured intensity of the characteristic 778 cm^{-1} peak of DMCHA against the DMCHA mass initially injected. The black dashed line represents the linear fitting used for extrapolations. DMCHA, *N,N*-dimethylcyclohexylamine.

peak follows a linear relationship with the DMCHA concentration in the range of 0.5–2.7 g/L. For as low as 0.4 and 0.3 g/L of DMCHA in toluene, the peak is still detectable. However, the intensity of the characteristic peak deviated from the linear fitting, thus setting the limit of quantification (LOQ) at 0.5 g/L. The residual characteristic peak cannot be distinguished from the noise at 0.15 g/L, so the limit of detection (LOD) is set at 0.3 g/L. In the linear range from 0.5 to 2.7 g/L of DMCHA, the intensity of the 778 cm^{-1} peak after extraction can be used to quantify the residual DMCHA peak by

matching the intensity of the characteristic peak to the DMCHA mass through this calibration curve.

To quantify the residue in the PS particles prepared from emulsion extraction, we followed our extraction method to separate the residual solvent from polystyrene. The filtered polystyrene with trapped solvent is washed by an acid solution, dried, and then dissolved in toluene. The aqueous extractant phase is then analyzed using Raman spectroscopy and the residue is quantified using the established calibration curve in Figure 1e.

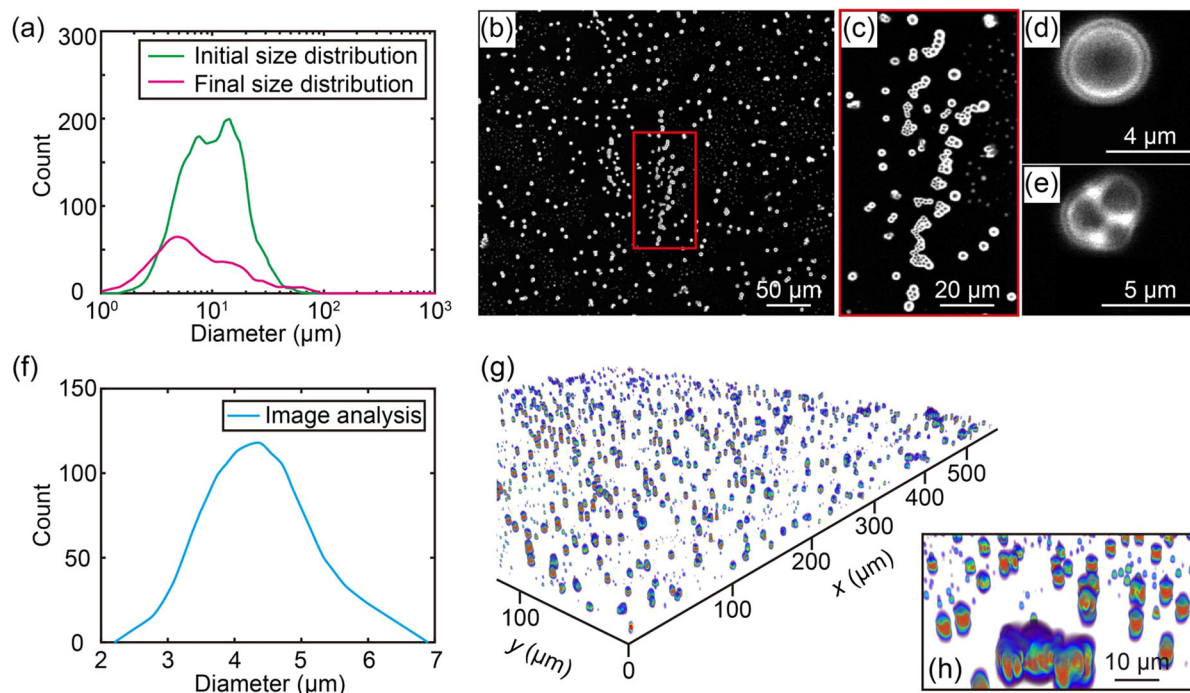


FIGURE 2 Size distribution of emulsion and polystyrene particle before and after the extraction process. (a) Comparison of the size distribution measured via FBRM of the initial emulsion (80:20 wt% aqueous:organic phase ratio at $T = 20^{\circ}\text{C}$) before trigger addition (2.5 M formic acid solution added in 120 min) and final polystyrene dispersion. (b) Typical confocal microscopy image of a redispersed polystyrene powder resulting from the extraction of SHS from the emulsion. (c) Close-up of aggregated particles in the powder. (d) Zoomed view of a single polystyrene particle. (e) Zoomed view of a particle cluster composed of three smaller particles merged together. (f) Size distribution of the powder shown in (b) measured via image analysis. (g) Three-dimensional map of the produced polystyrene powder created by confocal microscopy imaging. (h) Close-up of aggregated particles in the 3D map. DMCHA, *N,N*-dimethylcyclohexylamine.

Figure 2a shows the initial emulsion droplet size distribution obtained by a focused beam reflectance measurement (FBRM) before the addition of the trigger. A typical droplet size has been found to be between 5 and 30 μm . After the extraction of the switched SHS from the emulsion, polystyrene particles separate out and the size of the final polystyrene dispersion decreases to the range of 1–20 μm . The particle count decreases after the addition of the trigger, possibly due to drop coalescence during the trigger addition and/or agglomeration of the final polystyrene particles. Additionally, the merging of particles can also result in the formation of larger particles.

Figure 2b shows a typical confocal image of a polystyrene powder obtained from emulsion extraction of the SHS after the powder was redispersed in ethanol. The particles appear to be isolated spheres or aggregates as shown in Figure 2c. Figure 2d shows a zoomed view of a 4 μm particle, while Figure 2e shows a zoomed view of a 5 μm particle cluster consisting of three particles. The size of the particles obtained from the image is shown in Figure 2f and ranges from about 2 to 7 μm , with a mean diameter of $4.3 \pm 0.9 \mu\text{m}$. The particle size is consistent with the size distribution measured via FBRM. Large particles were also found from FBRM measurements, possibly due to clusters in the mixture. Figure 2g shows a 3D image of the particles, and Figure 2h shows a close-up of one large particle cluster 25 μm in length.

In earlier work,²⁰ similar aggregates were found in the latexes resulting from emulsion extraction of an SHS. During the process of switching, an acid is added that partially reacts with the SHS to form a salt. A consequence of the acid addition and salt formation is an increase in the ionic strength of the aqueous medium, which may lead to the compression of the electric double layer, thus enhancing the likelihood of aggregation of the hydrophobic particles.

We conducted a range of experiments to study the influence of the total trigger addition duration on the residual solvent. For this set of experiments, we followed Condition No. 1 described in Table 1. The total volume of the trigger solution added to the emulsion was maintained constant; therefore, an increase in the addition rate resulted in a shorter trigger addition duration. The trigger addition rate changed from 0.1 to 8 mL/min, resulting in the switching duration ranging from 7.5 to 600 min.

Figure 3a shows the reproducibility of the characteristic peak of DMCHA for five Raman measurements on one sample. Figure 3b shows the Raman characteristic peak of DMCHA measured in the aqueous phase after extraction for different trigger addition durations. The intensity is normalized by the powder weight to take into account the sample mass effect. The Raman characteristic peak is nearly independent of the total trigger addition duration.

Figure 3c shows the DMCHA residue against the total trigger addition duration. Each point represents one sample, and the error

TABLE 1 The experimental parameters studied for the effects from the formic acid trigger.

No.	Total trigger addition duration (min)	Formic acid concentration (M)	Organic fraction emulsion (wt%)	Temperature (°C)
1	7.5, 15, 30/60/80/120/240/600	2.5	20	20
2	120	2.5/3.1/3.8/4.4/5	20	20
3	120	2.5	10/15/20/25/30	20
4	120	2.5	20	15/20/30/35/40/50/60/70/90

Note: The parameters in the experiments are formic acid concentration in the solution, total trigger addition duration, emulsion composition, and emulsion temperature.

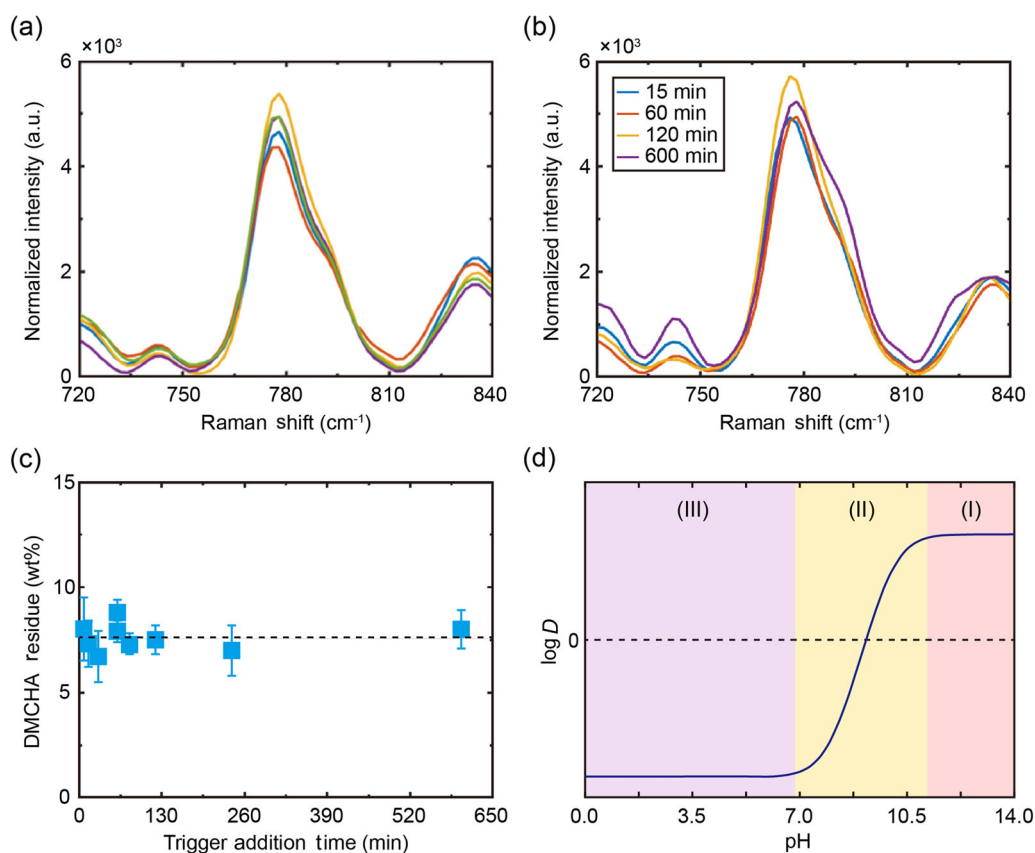


FIGURE 3 Raman spectra analysis of the DMCHA residue in the aqueous phase after extraction with varying trigger addition durations. (a) Characteristic peak of DMCHA from 5 measurements after extraction of the sample on the basis of Condition No. 1 in Table 1 for a total trigger addition duration of 120 min. (b) DMCHA characteristic peak for powders from different total trigger addition durations (Condition No. 1, Table 1). (c) Plot of the DMCHA residue against the total trigger addition duration. Each point represents one powder sample. The error bar represents the standard deviation over 5 Raman measurements. A constant DMCHA residue of 7.6 ± 0.6 wt% is found with varying trigger addition durations. (d) Sketch of the distribution coefficient of an SHS between an organic and aqueous phase against the pH of the aqueous phase. Area (I) corresponds to high pH, before the addition of the trigger. Area (II) shows the range of the pH characteristic of the switching process where DMCHA starts to protonate. Area (III) corresponds to the low-pH region, where most DMCHA will remain in the aqueous phase. DMCHA, *N,N*-dimethylcyclohexylamine.

bar represents the standard deviation from five Raman spectroscopy measurements. The residual DMCHA found in the powder is nearly constant with the trigger addition rate. According to the Raman characteristic peak, the average DMCHA residue found in the powder is 7.6 ± 0.6 wt%. This residue is close to what was reported for polystyrene foam recycling using DMCHA in previous work.²

The driving force for the transfer of DMCHA between phases during switching can be described by its distribution coefficient.³⁵ The distribution coefficient of DMCHA is defined as the ratio between the DMCHA concentration in the organic phase and in the aqueous phase:

$$D = \frac{[\text{DMCHA}^0]_{\text{org}} + [\text{DMCHAH}^+]_{\text{org}}}{[\text{DMCHA}^0]_{\text{aq}} + [\text{DMCHAH}^+]_{\text{aq}}} \quad (1)$$

$[\text{DMCHA}^0]_{\text{org}}$ and $[\text{DMCHAH}^+]_{\text{org}}$ are the concentrations in the organic phase of the neutral and protonated forms of DMCHA, respectively. Similarly, $[\text{DMCHA}^0]_{\text{aq}}$ and $[\text{DMCHAH}^+]_{\text{aq}}$, respectively, are the concentrations in the aqueous phase of the neutral and protonated forms of DMCHA.

In our experiments, DMCHA is in equilibrium between an organic phase containing polystyrene and an aqueous phase containing the trigger solution. During the switching of the emulsion, the pH of the aqueous phase steadily decreases. As neutral DMCHA is converted into protonated DMCHA through an acid–base reaction, the distribution coefficient is directly dependent on the pH of the aqueous phase. Figure 3d shows the sketch of a distribution coefficient against the pH of the aqueous phase, as it was modeled in previous work.³⁵ Area (I) corresponds to the high-pH region at the beginning of our experiment, where DMCHA is mostly present in the organic phase. At high pH, D can be simplified by the partition coefficient of the neutral form of DMCHA K .

$$K = \frac{[\text{DMCHA}^0]_{\text{org}}}{[\text{DMCHA}^0]_{\text{aq}}}, \quad (2)$$

K is therefore constant with pH change. As the trigger solution is added, the pH of the aqueous phase starts decreasing and reaches area (II). This region corresponds to the switching of DMCHA from hydrophobic (neutral form) to hydrophilic (protonated form), where DMCHA transfers from the organic phase to the aqueous phase. After switching, the aqueous phase reaches the low-pH area (III), where D reaches a plateau. In this region, D can be simplified by the partition coefficient of the protonated form of DMCHA K'

$$K' = \frac{[\text{DMCHAH}^+]_{\text{org}}}{[\text{DMCHAH}^+]_{\text{aq}}}. \quad (3)$$

The distribution coefficient describes the equilibrium that would occur, given sufficient time. However, mass transfer from within the emulsion drop to the organic–aqueous interface can delay the

approach to equilibrium. As DMCHA is extracted from the emulsion drop, the PS will be enriched, increasing the viscosity of the drop and decreasing the mobility of the remaining DMCHA. As further DMCHA is extracted, the PS will precipitate, creating a physical barrier to diffusion. Both these effects might be expected to be strongest near the drop surface, potentially trapping DMCHA and water in the drops. Therefore, the trigger solution addition rate will affect how fast the emulsion switches that might be expected to influence the removal of DMCHA from the emulsion drops and so the residual concentration in the final PS powder. However, within the ranges of addition rates tested, no significant effect was noted.

Another series of experiments was performed to examine the influence of the trigger solution concentration on the DMCHA residue. Condition No. 2 from Table 1 was followed. The total volume of the trigger solution added was 60 mL, but the concentration of formic acid in the solution was changed from 2.5 to 5 M.

Figure 4a shows the Raman spectra of the aqueous phase resulting from the extraction at different trigger solution concentrations. The intensity is normalized by the mass of the powder sample. Similar to the trigger addition rate, the characteristic peak intensity is weakly dependent on the trigger concentration. Figure 4b shows the extrapolated DMCHA residue from the calibration curve. The DMCHA residue is nearly constant with changing formic acid concentration. An average DMCHA residue of 7.5 ± 0.3 wt% is found in the polystyrene powders.

The observed result can be partially explained by the distribution coefficient at equilibrium. At the final low pH, the equilibrium DMCHA residue after switching is proportional to the distribution coefficient. In the low-pH region, the distribution coefficient is constant and equal to the partition coefficient of the protonated form of DMCHA K' . On increasing the trigger solution concentration, the final pH of the aqueous phase decreases, which does not shift the distribution coefficient. Delivering a higher concentration of switching solution at the same time will result in a faster switching rate, but

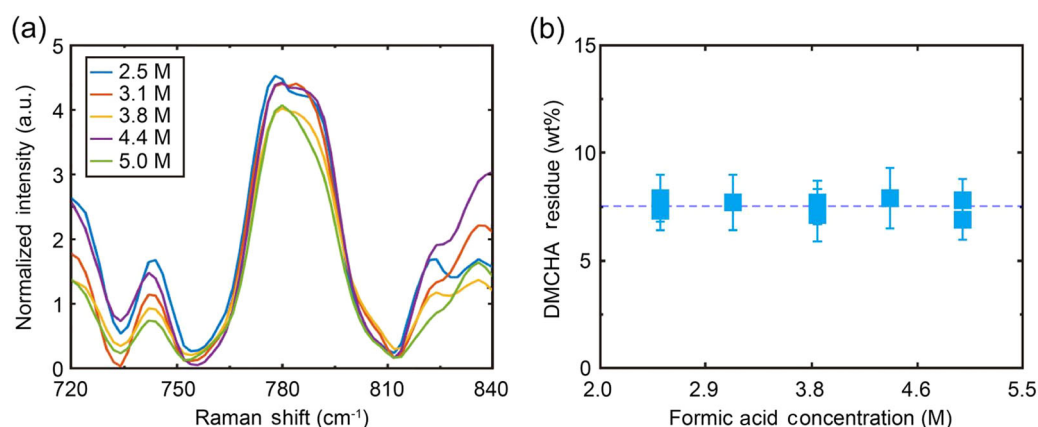


FIGURE 4 Raman spectra analysis of the DMCHA residue in the aqueous phase following extraction at various trigger solution concentrations. (a) DMCHA characteristic peak of the extractant aqueous phase after extraction from the powder samples prepared with different trigger solution concentrations. The organic fraction was maintained constant at 20 wt%, while formic acid solutions were used as the trigger and added in 120 min. The temperature was maintained at 20°C. (b) Plot of the DMCHA residue against the trigger solution concentration. The error bars represent the standard deviation over five Raman measurements. DMCHA, *N,N*-dimethylcyclohexylamine.

as shown previously, over the range of addition rates tested here, no change was observed in the level of the DMCHA residue in the particles.

The emulsion composition was varied to investigate the change in the DMCHA solvent residue in the resultant powder. The temperature, trigger addition rate, and trigger concentration were all maintained constant throughout this set of experiments. In all experiments, the total amount of the acid added to water is always sufficient to switch all DMCHA in the system. Figure 5a shows the Raman peak at 778 cm^{-1} for powder made from emulsion with different organic phase fractions. Condition No. 3 was used for this set of experiment. The range of organic phase fraction studied was between 10 and 30 wt%.

In this experiment, the detected Raman characteristic peak depends on the organic phase fraction used for the emulsion preparation. A smaller organic phase fraction resulted in an increased intensity of the

Raman characteristic peak of DMCHA. Figure 5b shows the residual DMCHA, which is found to decrease with an increase in the organic phase fraction. At 10 wt% of the organic phase fraction, the DMCHA residue in the resulting polystyrene powder was $19.2 \pm 1.6\text{ wt}\%$. However, at a higher organic phase fraction, the resulting residual solvent in the powder was reduced to $5.7 \pm 0.8\text{ wt}\%$. Emulsions with an organic phase fraction lower than 10 wt% or higher than 30 wt% were unstable and no powder was formed. A similar effect of the organic to aqueous phase ratio on the residual solvent has previously been reported for the extraction of bitumen with TEDPA.²¹

The effect from the organic phase fraction could be related to water trapped in the PS particles. Protonated DMCHA dissolved in water microdroplets may be left in the particles after extraction. We noticed water present in the particle powder. Figure 5c shows the photo of the toluene phase after dissolution of the produced polystyrene. During the polystyrene dissolution, the toluene phase

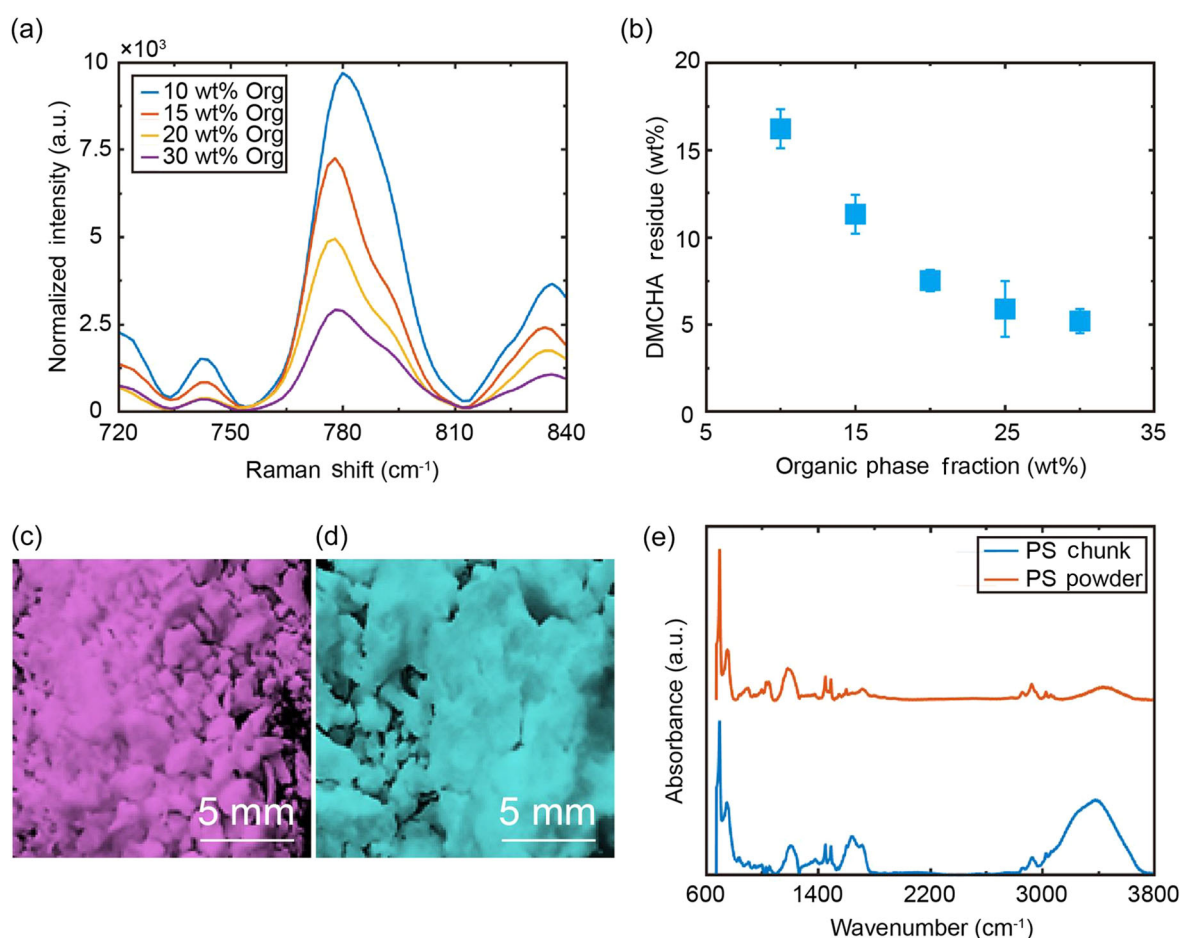


FIGURE 5 Raman spectra analysis of the DMCHA residue in the aqueous phase following extraction with various organic phase fractions. (a) DMCHA characteristic peak of the extractant aqueous phase after extraction from the powder made from emulsion with different organic phase fractions. 2.5 M of formic acid solution was used as the trigger, added over 120 min. The temperature of the emulsion was 20°C. (b) Plot of the DMCHA residue against the organic fraction in the emulsion. Each point represents one powder sample, and the error bar represents the standard deviation over five Raman measurements. (c, d) Images of recovered polystyrene from a 10 wt% organic phase emulsion switched at 20°C with a 2.5 M formic acid solution. (c) Polystyrene recovered in powder form. (d) Polystyrene recovered as a solid chunk. (e) Corresponding FTIR measurement of the polystyrene powder and chunk. Both samples show the characteristic bands of water, especially in the polystyrene chunk. DMCHA, *N,N*-dimethylcyclohexylamine.

becomes cloudy, and a second minor immiscible water phase can be detected at the bottom of the toluene phase. The presence of the cloudy phase indicates the existence of water microdroplets as an emulsion, which may be stabilized by residual SDS in the powder. Protonated DMCHA is also a compound with surface activity that may stabilize water microdroplets in dissolving a nonswitched drop.

On decreasing the organic phase content under 20 wt% in the emulsion, some of the polystyrene was recovered as a solid chunk, as shown in Figure 5d. Nearly 50 wt% of the polystyrene was recovered as powder, while the remaining polystyrene was aggregated in the form of a polystyrene chunk for 10 wt% of the organic phase in the emulsion. The higher organic phase fraction would result in a higher final concentration of switched DMCHA in the aqueous phase and one possibility is that this may act as a surfactant and stabilize the PS particles and inhibit their agglomeration.

Figure 5e shows the FTIR absorbance spectra of both the polystyrene powder and the polystyrene chunk. In both cases, typical water bands due to vibrations of the O–H bond were observed at 3000–3500 and 1500–1700 cm^{-1} . However, the magnitudes of the water bands were higher in the polystyrene chunk. More water was therefore trapped during the polystyrene chunk formation, leading to higher DMCHA residue in the recovered polystyrene.

The fraction of water contained in dissolving DMCHA drops could be much higher than the solubility of water in DMCHA (~21 wt% at

20°C³⁶), as a large number of dispersed microdroplets were present in the DMCHA-PS drops.³⁷ Recent research showed that the solubility of a compound in a drop may be markedly different from the solubility in the bulk, when a phase separation process or chemical reactions in the drops may lead to a large change in the concentration of the compound in the small drops.^{38,39} Moreover, for water microdroplets to escape from the dissolving drop and merge into the surrounding liquid phase, their transport through the interface has to take place, which may be hindered by high viscosity near the interface by accumulated PS. Therefore, the residue of DMCHA trapped in water microdroplets is likely much higher than that estimated from the solubility of water in a nonswitched solvent in bulk. Additionally, DMCHA in water microdroplets may be in a protonated form due to the presence of acid, which further increases the residue of DMCHA trapped in PS particles.

The effect of the temperature at which the switching of the emulsion occurs was also studied under Condition No. 4 shown in Table 1. The temperature was maintained constant using a water bath along with constant mixing at 300 rpm. A temperature difference of 0.5°C was observed between the bottom and top of the emulsion.

Figure 6a shows the Raman spectra of DMCHA normalized by the sample mass after extraction from the powders for different temperatures. The temperatures studied ranged from 15°C to 90°C. The normalized intensity of the DMCHA characteristic peak increases with

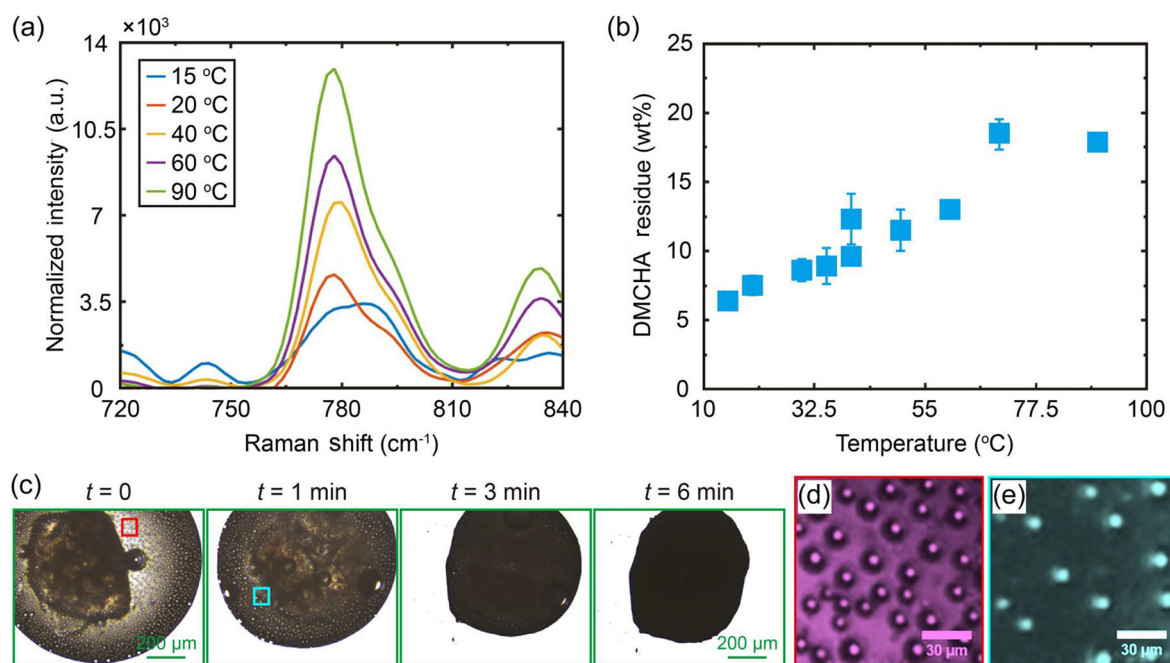


FIGURE 6 Raman spectra analysis of the DMCHA residue in the aqueous phase following extraction at different temperatures. (a) DMCHA characteristic peak of the extractant aqueous phase after extraction for powders prepared at different temperatures. The organic fraction was maintained constant at 20 wt%. 2.5 M of formic acid solution was used as the trigger, added over 120 min. (b) Plot of the DMCHA residue against the emulsion temperature for different powders. Each point represents one powder sample, and the error bar represents the standard deviation over five Raman measurements. The DMCHA residue is found to increase with the temperature from 6.3 wt% at 15°C to 17.8 wt% at 90°C. (c) Snapshots of a single sessile 90/10 DMCHA/polystyrene drop in a 0.1 M formic acid solution bath at 90°C observed using an upright optical microscope during the extraction process of the drop. A phase separation behavior is observed with precipitated polystyrene at the center of the drop and water droplets in the DMCHA-rich phase of the drop. On the right, the final polystyrene particle is shown. (d, e) Expanded view of water droplets observed in the DMCHA/polystyrene drop. DMCHA, *N,N*-dimethylcyclohexylamine.

an increase in temperature, suggesting a higher DMCHA residue as the temperature increases. Figure 6b shows the DMCHA residue extrapolated from the calibration curve. The DMCHA residue increases from 6.3 wt% at 15°C to 17.8 wt% at 90°C.

An increase in the DMCHA residue had previously been reported during lipid extraction from microalgae.¹⁵ Two reasons can be suggested to explain the increase in the residue content at higher temperatures. First, the distribution coefficient of DMCHA between polystyrene and water may be affected by the temperature. At low pH, as most of the DMCHA is protonated, the distribution coefficient is reduced to the partition coefficient of protonated DMCHA. Higher temperatures may improve the solubility of charged DMCHA in the polystyrene phase relative to the solubility in the aqueous phase.^{40,41}

Second, higher temperatures may also increase the intake of water into DMCHA, leading to a higher amount of trapped water in the droplet. The higher intake of water may be related to multiple physiochemical properties that are sensitive to temperature, for example, mutual solubilities of DMCHA and water, switching dynamics, viscosity, diffusion coefficients, or interfacial tension. It is evident from the experiments that more water droplets are formed at higher temperatures. Figure 6c shows snapshots of a dissolving 90:10 wt% DMCHA/polystyrene sessile drop in a 0.1 M formic acid trigger bath at a high temperature of 90°C. During this experiment, the DMCHA is solubilized by switching similarly to the emulsion extraction process. In this experiment, polystyrene precipitates at the center of the drop, similar to the observed precipitated polystyrene during the emulsion formation. Water droplets are observed to move freely in the DMCHA-rich phase. Figure 6d,e shows a zoomed view of some of the water droplets observed. As the drop shrinks, the water droplets follow the movement of the drop boundary. Some water droplets remain trapped in the polystyrene particle after the DMCHA drop dissolution.

This phase separation behavior has been observed at room temperature in previous work.³⁷ Similarly, water droplets are observed following the shrinking interface of the drop. At the end of the dissolution process, the increase of the viscosity of the drop fixes the water droplets that remain trapped in the particle. However, at high temperatures, larger and more water droplets can be observed. Increased trapped water phase in the high-temperature case may store more protonated DMCHA, resulting in more residual solvents in the particles.

We investigate the influence of trigger type on the residual DMCHA in polystyrene after switching DMCHA from emulsions. The triggers studied are formic acid, sulfuric acid, and dry ice. The pH of the three triggers is set at 5.6, which is consistent with that of CO₂-saturated water. Figure 7a–c shows pictures of the recovered polystyrene for each trigger type. For the formic acid (Figure 7a) and sulfuric acid (Figure 7b) triggers, the experiments yield a powder. However, for the dry ice trigger, Figure 7c, polystyrene is recovered as a single aggregate.

Figure 7d shows the DMCHA residue in the recovered polystyrene. Unwashed samples yielded a high DMCHA residue of around 15 wt%; however, it was shown that adding an acidic phase washing step could reduce the DMCHA residue by 4 wt% in the sulfuric acid case to 7.5 wt% for the formic acid trigger. The

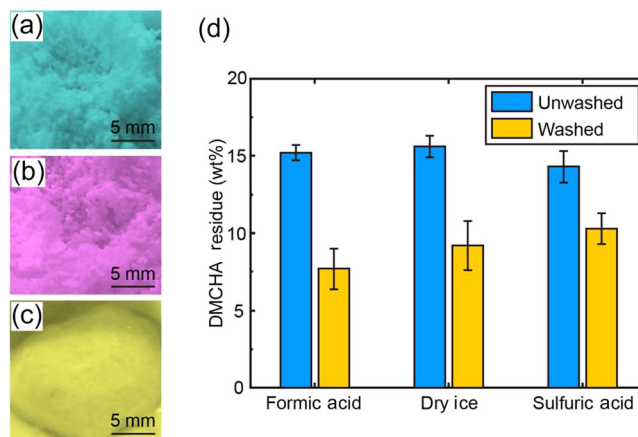


FIGURE 7 DMCHA residue with different trigger types. Artificial colored images of the polystyrene recovered with (a) formic acid, (b) sulfuric acid, and (c) dry ice. (d) DMCHA residue for formic acid, dry ice, and sulfuric acid, with and without the acid washing step by a 0.9 M sulfuric acid solution. The error represents the standard deviation over five Raman spectroscopy measurements. The washing step removed DMCHA that was present on the surface of the powders. DMCHA, *N,N*-dimethylcyclohexylamine.

difference in the residue between washed and unwashed samples can be attributed to the residual DMCHA present on the surface of the recovered polystyrene. The acidic washing solution can solubilize the surface DMCHA during the washing step, contributing to a reduction in the final residue.

For washed samples, the sulfuric acid trigger yielded polystyrene with 10.3 ± 1.0 wt% residual DMCHA, dry ice yielded polystyrene with 9.2 ± 1.6 wt% DMCHA, and formic acid yielded polystyrene powder with 7.7 ± 1.3 wt% DMCHA. There is a slight influence of the trigger type on the residual DMCHA; however, Student's *t*-test showed that only the residual DMCHA between the formic and sulfuric acid trigger was significant. The different cations present during the switching of DMCHA from the emulsion might explain the differences in the DMCHA residue between the two triggers. The different cations may influence the distribution coefficient and therefore change the residual DMCHA observed.⁴² In previous work on pharmaceutical compounds, salt has also been found to influence the distribution coefficient.⁴³ However, this effect is still small in magnitude to the one observed for the temperature and emulsion composition.

CONCLUSIONS

In this work, polystyrene microparticles were prepared by dissolution of SHS from emulsion droplets containing polystyrene and an SHS initially in the hydrophobic state. An acidic aqueous solution was used as the trigger to switch the SHS to the water-soluble state. The residual SHS in the polystyrene microparticles was quantified by Raman spectroscopy after extraction from dissolved particles. Our results showed that the residual SHS remained constant at 7.6 ± 0.5 wt% of the recovered powder with varying trigger addition rates and trigger concentrations.

However, the SHS residue level changed with trigger types used to switch DMCHA, attributed to the influence of different cations on the distribution coefficient of the SHS in water and in the organic phase.

Importantly, on decreasing the organic phase fraction from 30 to 10 wt%, the SHS residue was found to increase from 5.2 to 16.2 wt%, while an increase in temperature from 15 to 90°C also led to an increase in the residual SHS from 6.3 to 17.8 wt%. The higher residue at higher temperatures may be related to the presence of more trapped water in the recovered polystyrene particles due to increased agglomeration at high temperatures and with a low organic phase fraction. The confined water microdroplets may carry the SHS in the water-soluble form, possibly leading to a high SHS residual in the final particle product. The correlation between the residue content and water trapped in the emulsion drops is an aspect that has not been considered before. Our work may suggest that a possible approach to tackle a low solvent residue may be to reduce the water entrapped in the emulsion droplets.

METHODS

SHS/polymer solution was prepared using a 90:10 wt% mixture of DMCHA (Sigma-Aldrich; 99%) and polystyrene (Sigma-Aldrich, $M_w = 40,000$ g/mol, beads, 99%). Both chemicals were mixed at room temperature in sealed vials for 2 h, resulting in complete dissolution of the polystyrene. The aqueous phase was prepared using a 3 wt% solution of sodium dodecyl sulfate (Sigma-Aldrich, 98.5%, SDS, surfactant) in (Milli-Q) water. In a typical emulsion formation, a controlled amount of organic phase, 6–18 g of 90:10 DMCHA:polystyrene solution, was added to the aqueous phase, and 54–42 g of 97:3 SDS solution. The organic phase fraction was used as a studied parameter and ranged from 10 to 30 wt% of the total emulsion weight. The organic phase was slowly added to the aqueous phase under magnetic stirring at 300 rpm to form a milky emulsion. Some polystyrene precipitated during the emulsion production and was removed before emulsion switching. The precipitated polystyrene was attributed to the high water solubility in DMCHA, measured to be 18.3 ± 0.8 vol%. Water acts as a polystyrene nonsolvent, decreasing its solubility in the DMCHA phase and causing polystyrene precipitation.

Formic acid (Sigma-Aldrich; 95%) and sulfuric acid (Thermo Fisher Scientific, 95%) solutions as well as dry ice were used as triggers to switch the emulsion. Acidic solutions were freshly prepared before each experiment in sealed vials under magnetic stirring for 10 min. Sulfuric acid solutions (1 M) were left to cool down to ambient temperature before usage. As shown in Figure 1, a fixed volume of DMCHA/polystyrene emulsion (60 mL) was placed in a beaker under magnetic stirring at 300 rpm, while the same volume of trigger solution (60 mL) was loaded into a plastic syringe. The acidic solutions were then added at a controlled rate using a syringe pump until complete depletion of the syringe. For dry ice, small pieces of ice (1 g) were progressively added every 2 min to the emulsion until 40 g of ice was introduced. The emulsion was kept

partially sealed to prevent any pressure build-up. The temperature of the emulsion was controlled using a water bath, and the temperature of the emulsion was measured using a thermocouple to ensure the homogeneity of the temperature within the emulsion. For the formic acid trigger solution, the study parameters include the solution concentration, the total trigger addition duration, the organic fraction in the emulsion, and the emulsion temperature. The parameters are listed in Table 1. The majority of the polystyrene was recovered as a powder during the emulsion-switching process. However, in some situations, such as when the temperature was high or the amount of organic phase in the emulsion was minimal, polystyrene aggregates developed along with the powder. In these situations, the resultant solid polystyrene chunk could account for up to 50 wt% of the recovered polystyrene.

Once the trigger solution addition was completed and the solvent was switched, the polystyrene dispersion was filtered using vacuum filtration (Q2 filter paper, Fisherbrand, particle retention $>2 \mu\text{m}$) to recover a polystyrene powder. The powder was washed using 100 mL of a 0.9 M sulfuric acid solution to eliminate the DMCHA left at the surface of the polystyrene powder. The powder was then left to dry for 24 h at room temperature. For imaging purposes, a trace amount of Nile red (Thermo Fisher Scientific, 99%) was used to dye the organic phase of the emulsion. The resulting powder could therefore be imaged under a Confocal Laser Scanning Microscope (DMI8 S, Leica Microsystems) with a $\times 20$ dry objective. The size distribution of the initial emulsion and the final dispersion was collected using a Focused Beam Reflectance Measurement probe (FBRM G400, Mettler Toledo).

To quantify the solvent residue in the powder, DMCHA was extracted from the polystyrene into an acidic aqueous phase. First, the polystyrene powder was weighed on a microbalance and then dissolved into 40 mL of toluene in a beaker under magnetic stirring. Second, 5 mL of a 0.9 M sulfuric acid solution was added as the extracting phase for DMCHA from the toluene phase. The two-phase mixture was then allowed to mix for 8 h. Once the mixing stopped and phase separation was completed, 3 mL of the aqueous phase was transferred to a vial. The aqueous phase was then analyzed in the vial using a handheld Raman spectrometer device (Cora 100, Anton Paar, 785 nm). The intensity was maintained at high settings with a 20 s exposure time. The results were then exported and baseline-corrected using splines to fit to the baseline. The measured residue content in wt% was obtained after the intensity is normalized by the mass of polystyrene powder.

ACKNOWLEDGMENTS

We are grateful for inspiring discussions with Dr Hassan Hamza in BC Research throughout the entire program. The authors acknowledge the funding support from the Mitacs Accelerate Program, the Canada Foundation for Innovation (CFI), the Natural Science and Engineering Research Council of Canada (NSERC), and Alberta-innovates. This work was partially supported by the Canada Research Chairs program. We are grateful for the technical assistance from IOSI Labs at the Faculty of Engineering, University of Alberta.

CONFLICT OF INTEREST STATEMENT

BC Research is a wholly owned subsidiary of NORAM Engineering and Constructors Ltd., which licensed the SHS technology platform originally developed and Patented at Queens University and are together developing new commercial applications for the SHS technology.

ORCID

Binglin Zeng  <http://orcid.org/0000-0002-7172-5557>

Xuehua Zhang  <https://orcid.org/0000-0001-6093-5324>

REFERENCES

- Jessop PG, Phan L, Carrier A, Robinson S, Dürr CJ, Harjani JR. A solvent having switchable hydrophilicity. *Green Chem.* 2010;12:809-814.
- Jessop PG, Kozycz L, Rahami ZG, et al. Tertiary amine solvents having switchable hydrophilicity. *Green Chem.* 2011;13:619-623.
- Yilmaz E, Soylyak M. Switchable polarity solvent for liquid phase microextraction of Cd (II) as pyrrolidinedithiocarbamate chelates from environmental samples. *Anal Chim Acta.* 2015;886:75-82.
- Lasarte-Aragón G, Lucena R, Cárdenas S, Valcárcel M. Use of switchable solvents in the microextraction context. *Talanta.* 2015;131:645-649.
- Ezoddin M, Abdi K, Lamei N. Development of air assisted liquid phase microextraction based on switchable-hydrophilicity solvent for the determination of palladium in environmental samples. *Talanta.* 2016;153:247-252.
- Shahraki S, Ahmar H, Nejati-Yazdinejad M. Electrochemical determination of nitrazepam by switchable solvent based liquid-liquid microextraction combined with differential pulse voltammetry. *Microchem J.* 2018;142:229-235.
- Oenning AL, Birk L, Eller S, de Oliveira TF, Merib J, Carasek E. A green and low-cost method employing switchable hydrophilicity solvent for the simultaneous determination of antidepressants in human urine by gas chromatography-mass spectrometry detection. *J Chromatogr B.* 2020;1143:122069.
- Behpour M, Nojavan S, Asadi S, Shokri A. Combination of gel-electromembrane extraction with switchable hydrophilicity solvent-based homogeneous liquid-liquid microextraction followed by gas chromatography for the extraction and determination of antidepressants in human serum, breast milk and wastewater. *J Chromatogr A.* 2020;1621:461041.
- Shahvandi SK, Banitaba MH, Ahmar H. Development of a new pH assisted homogeneous liquid-liquid microextraction by a solvent with switchable hydrophilicity: application for GC-MS determination of methamphetamine. *Talanta.* 2018;184:103-108.
- Moghadam AG, Rajabi M, Hemmati M, Asghari A. Development of effervescence-assisted liquid phase microextraction based on fatty acid for determination of silver and cobalt ions using micro-sampling flame atomic absorption spectrometry. *J Mol Liquids.* 2017;242:1176-1183.
- Vakh C, Pochivalov A, Andruch V, Moskvina L, Bulatov A. A fully automated effervescence-assisted switchable solvent-based liquid phase microextraction procedure: liquid chromatographic determination of ofloxacin in human urine samples. *Anal Chim Acta.* 2016;907:54-59.
- Phan L, Brown H, White J, Hodgson A, Jessop PG. Soybean oil extraction and separation using switchable or expanded solvents. *Green Chem.* 2009;11:53-59.
- Viner KJ, Roy HM, Lee R, He O, Champagne P, Jessop PG. Transesterification of soybean oil using a switchable-hydrophilicity solvent, 2-(dibutylamino) ethanol. *Green Chem.* 2019;21:4786-4791.
- Holland A, Wechsler D, Patel A, Molloy BM, Boyd AR, Jessop PG. Separation of bitumen from oil sands using a switchable hydrophilicity solvent. *Can J Chem.* 2012;90:805-810.
- Boyd AR, Champagne P, McGinn PJ, MacDougall KM, Melanson JE, Jessop PG. Switchable hydrophilicity solvents for lipid extraction from microalgae for biofuel production. *Bioresource Technol.* 2012;118:628-632.
- Du Y, Schuur B, Kersten SR, Brilman DW. Opportunities for switchable solvents for lipid extraction from wet algal biomass: an energy evaluation. *Algal Res.* 2015;11:271-283.
- Huang W-C, Liu H, Sun W, Xue C, Mao X. Effective astaxanthin extraction from wet *Haematococcus pluvialis* using switchable hydrophilicity solvents. *ACS Sustain Chem Eng.* 2018;6:1560-1563.
- Fu D, Farag S, Chaouki J, Jessop PG. Extraction of phenols from lignin microwave-pyrolysis oil using a switchable hydrophilicity solvent. *Bioresource Technol.* 2014;154:101-108.
- Samori C, Cespi D, Blair P, et al. Application of switchable hydrophilicity solvents for recycling multilayer packaging materials. *Green Chem.* 2017;19:1714-1720.
- Su X, Jessop PG, Cunningham MF. Preparing artificial latexes using a switchable hydrophilicity solvent. *Green Chem.* 2017;19:1889-1894.
- Yang Y, Sui H, Ma J, He L, Li X. Revealing the residual mechanism of switchable solvents in heavy oil. *Fuel Process Technol.* 2021;218:106857.
- Yip E, Cacioli P. The manufacture of gloves from natural rubber latex. *J Allergy Clin Immunol.* 2002;110:S3-S14.
- Weiss KD. Paint and coatings: a mature industry in transition. *Prog Polymer Sci.* 1997;22:203-245.
- Winnik MA. Latex film formation. *Curr Opin Colloid Interface Sci.* 1997;2:192-199.
- Vanderveen JR, Durelle J, Jessop PG. Design and evaluation of switchable-hydrophilicity solvents. *Green Chem.* 2014;16:1187-1197.
- Durelle J, Vanderveen JR, Quan Y, Chalifoux CB, Kostin JE, Jessop PG. Extending the range of switchable-hydrophilicity solvents. *Phys Chem Chem Phys.* 2015;17:5308-5313.
- Samori C, Pezzolesi L, Barreiro DL, Galletti P, Pasteris A, Tagliavini E. Synthesis of new polyethoxylated tertiary amines and their use as switchable hydrophilicity solvents. *RSC Adv.* 2014;4:5999-6008.
- Vanderveen JR, Geng J, Zhang S, Jessop PG. Diamines as switchable-hydrophilicity solvents with improved phase behaviour. *RSC Adv.* 2018;8:27318-27325.
- Cunha IT, McKeeman M, Ramezani M, et al. Amine-free CO₂-switchable hydrophilicity solvents and their application in extractions and polymer recycling. *Green Chem.* 2022;24:3704-3716.
- Irish DE, Chen H. Equilibria and proton transfer in the bisulfate-sulfate system. *J Phys Chem.* 1970;74:3796-3801.
- Irish D, Chen H. Raman spectral study of bisulfate-sulfate systems. II. Constitution, equilibria, and ultrafast proton transfer in sulfuric acid. *J Phys Chem.* 1971;75:2672-2681.
- Tomikawa K, Kanno H. Raman study of sulfuric acid at low temperatures. *J Phys Chem A.* 1998;102:6082-6088.
- Poizat O, Guichard V, Buntinx G. Vibrational studies of reactive intermediates of aromatic amines. IV. Radical cation time-resolved resonance Raman investigation of N, N-dimethylaniline and N, N-diethylaniline derivatives. *J Chem Phys.* 1989;90:4697-4703.
- Ando RA, Matazo DR, Santos PS. Detailed analysis of the charge transfer complex N, N-dimethylaniline-SO₂ by Raman spectroscopy and density functional theory calculations. *J Raman Spectrosc.* 2010;41:771-775.
- Durelle J, Vanderveen JR, Jessop PG. Modelling the behaviour of switchable-hydrophilicity solvents. *Phys Chem Chem Phys.* 2014;16:5270-5275.

36. Stephenson RM. Mutual solubilities: water cyclic amines, water alkanolamines, and water polyamines. *J Chem Eng Data*. 1993;38: 634-637.
37. Billet R, Zeng B, Lockhart J, Gattrell M, Zhao H, Zhang X. Dissolution dynamics of a binary switchable hydrophilicity solvent-polymer drop into an acidic aqueous phase. *Soft Matter*. 2023;19:295-305.
38. Wei Z, Li M, Zeng H, Zhang X. Integrated nanoextraction and colorimetric reactions in surface nanodroplets for combinative analysis. *Anal Chem*. 2020;92:12442-12450.
39. Wei Z, You JB, Zeng H, Zhang X. Interfacial partitioning enhances microextraction by multicomponent nanodroplets. *J Phys Chem C*. 2022;126:1326-1336.
40. Ingram T, Mehling T, Smirnova I. Partition coefficients of ionizable solutes in aqueous micellar two-phase systems. *Chem Eng J*. 2013; 218:204-213.
41. Greminger DC, Burns GP, Lynn S, Hanson DN, King CJ. Solvent extraction of phenols from water. *Industr Eng Chem Process Design Dev*. 1982;21:51-54.
42. Chen C-S, Lin S-T. Prediction of pH effect on the octanol-water partition coefficient of ionizable pharmaceuticals. *Industr Eng Chem Res*. 2016;55: 9284-9294.
43. Ingram T, Richter U, Mehling T, Smirnova I. Modelling of pH dependent n-octanol/water partition coefficients of ionizable pharmaceuticals. *Fluid Phase Equilib*. 2011;305:197-203.

How to cite this article: Billet R, Zeng B, Wu H, et al. Hydrophilic solvent recovery from switched-on microdroplet dissolution. *Droplet*. 2023;2:e82. doi:10.1002/dro2.82